



Green  
Chemistry

**Materials for the Biorefinery: High Bio-content, Shape  
Memory Kraft Lignin-derived Non-Isocyanate Polyurethane  
Foams Using a Non-toxic Protocol**

Journal:	<i>Green Chemistry</i>
Manuscript ID	GC-ART-05-2020-001659.R2
Article Type:	Paper
Date Submitted by the Author:	29-Jul-2020
Complete List of Authors:	Sternberg, James; Clemson University College of Engineering Computing and Applied Sciences, Automotive Engineering Pilla, Srikanth; Clemson University College of Engineering Computing and Applied Sciences, Automotive Engineering

SCHOLARONE™  
Manuscripts

**Materials for the Biorefinery: High Bio-content, Shape Memory Kraft Lignin-derived Non-Isocyanate Polyurethane Foams Using a Non-toxic Protocol.**

James Sternberg<sup>a,b</sup>, \*Srikanth Pilla<sup>a,b,c,d</sup>

<sup>a</sup> Clemson Composites Center, Clemson University, Greenville, SC 29607, United States

<sup>b</sup> Clemson University International Center of Automotive Research, 4 Research Dr., Greenville, SC 29607, United States

<sup>c</sup> Department of Material Science and Engineering, Clemson University, Clemson, SC 29634, United States

<sup>d</sup> Department of Mechanical Engineering, Clemson University, Clemson, SC 29634, United States

\*Corresponding Author: [spilla@clemson.edu](mailto:spilla@clemson.edu)

**Abstract**

Polyurethanes are among the top six polymers produced in the world and are widely used in the automotive, furniture, construction and appliance industry for their light weight, impact resistance, and insulating properties. However, the use of hazardous diisocyanates used in polyurethane formulations has led many to search for more sustainable alternatives. The use of the lignin component of biomass has been targeted to replace the often toxic and petroleum-derived precursors to polymer synthesis in support of the biorefinery concept where natural materials are used as feedstock for commodity plastics. The use of lignin is often hampered due to its low reactivity, heterogeneity and the necessity of employing extensive purification and/or functionalization measures to ensure materials of comparable quality. In this report, a unique method for the synthesis and processing of non-toxic, non-isocyanate polyurethane foam utilizing unmodified Kraft lignin and a biobased curing agent is presented. Raw Kraft lignin is functionalized with green organic carbonates and a non-toxic approach is taken to solubilize the precursors with a curing agent from

renewable fatty acids enabling rapid gel-times. For the first time, NIPU foams from lignin are synthesized while the structure-property relationships of different reaction mixtures is studied demonstrating shape memory capacity and a 100% biobased carbon content.

## **Introduction**

The demand for environmentally benign material synthesis has grown in recent decades supported by the green chemistry movement as well as the interest to replace petroleum derived chemicals with chemical precursors from biomass. The toxicity associated with petroleum resources as well as a desire to lower the overall carbon footprint of industrial processes has led efforts in support of the bio-refinery concept where natural materials are used as feedstock for chemical and material production. With the initial success of cellulosic ethanol production in the United States and elsewhere an increasing demand to valorize the lignin component in biomass has gained momentum due to the benefits of lowering the mean ethanol selling price (MESP) to compete with petroleum derived fuels. One promising way to valorize lignin is through the synthesis of polymers and materials that can replace the traditional petroleum derived route to polymer production and harness the world's most abundant source of aromatic carbon.<sup>1</sup> A survey of the literature surrounding polymers derived from lignin presents some truly innovative ways of using green chemistry approaches but unfortunately reveals that typical protocols still make use of harmful, toxic, and petroleum derived solvents and reagents lowering the biobased content and renewability of formulations.<sup>2-4</sup>

Lignin as a macromolecule has been used in a variety of applications, yet the success of using lignin as a polyol in polyurethane foam production is arguably its most advanced and researched initiative. Polyurethanes are one of the world's most versatile polymers finding applications in the automotive, aerospace, construction, furniture, coating and bearing industries to name a few.<sup>5</sup> This versatility is due in large part to the ease and efficiency of the reaction of polyols with diisocyanates to create flexible to rigid foams and plastic materials. Unfortunately, the use of diisocyanates have landed polyurethanes atop a list for the 50 most toxic polymers based on its own synthetic route making use of the deadly gas phosgene.<sup>6</sup> In addition, diisocyanates themselves have been labeled a "CMR" (Cancer causing, Mutagenic and Reproductive toxin) by the European community and have gained similar warnings in the United States.<sup>6</sup> The incorporation of lignin in polyurethane foams (PUFs) is a well-researched topic, showing that lignin can be used to replace traditional polyols used in the reaction with diisocyanates. Unfortunately, to synthesize materials with similar properties to conventional PUFs, propylene oxide (PO) must be used to simultaneously liquify lignin as well as extend nascent hydroxyl groups to create a more reactive lignin-derived precursor.<sup>7,8,9</sup> However, the toxicity and explosive hazard associated with PO has led researchers to look for a more benign route to lignin functionalization.

The use of organic carbonates has emerged as a sustainable source for the replacement of PO creating chain extended lignin derivatives with green alternatives such as ethylene carbonate,<sup>10</sup> propylene carbonate,<sup>11,12</sup> glycerol carbonate and others.<sup>13-15</sup> The use of organic carbonates has been shown to extend both aromatic and aliphatic hydroxyl

groups of lignin with etherified and carboxylated chains thus increasing the reactivity of lignin in light of synthesizing more functional polymers. In addition to the sustainable benefit of using organic carbonates, the unwanted homopolymerization of PO is avoided with the use of the well-controlled reaction of carbonates.<sup>14</sup> Despite the success of using organic carbonates for lignin functionalization, very few examples of lignin-derived polymers have used this method. For example, after functionalization with ethylene carbonate, Liu et al. esterified lignin with propionic acid creating a sustainable lignin-derived ester.<sup>10</sup>

Non-isocyanate polyurethanes can be synthesized through a variety of routes including polycondensation of carbamates and the ring opening reaction of bis-cyclic carbonates with diamines.<sup>16</sup> The use of cyclic carbonates is the most promising method producing no other chemical intermediates or by-products. The ring opening reaction creates additional hydroxyl groups within the NIPU structure often increasing the hydrolytic stability and chemical resistance of the polymers.<sup>17</sup> Cyclic carbonates are most often inserted on biobased precursors through epoxidation with the toxic reagent epichlorohydrin and subsequent carbonation using high pressure CO<sub>2</sub> and long reaction times.<sup>18</sup> However, a new technique for lignin cyclocarbonation has been submitted by the Lehnen group showing that organic carbonates can be used with Organosolv lignin to produce cyclocarbonated lignin with comparable results.<sup>19</sup>

The reaction between cyclocarbonates and diamines has been used for a variety of vegetable oils, tannins, and other biobased compounds yet the use of lignin in such materials is actually quite rare.<sup>20-23</sup> A few studies reporting on lignin-derived NIPUs have

resulted in very brittle structures, or low mechanical properties with evidence of unreacted precursor material. Lee et al. have reported on the use of cyclocarbonated soybean oil cured with aminopropyltriethoxysilane (APES).<sup>24</sup> Lignin was added to the polymer structure through the reaction of lignin-derived hydroxyl groups and APES. Unfortunately, the results showed low tensile strengths (~1 MPa) giving evidence to low the reactivity between lignin and APES. Salanti et al. have developed a protocol for the cyclocarbonation of the lignin precursor making it possible to derive the polyurethane linkage directly on the lignin macromolecular structure.<sup>25</sup> This protocol makes use of epichlorohydrin to epoxidize lignin followed by CO<sub>2</sub> insertion over 20 hours to form cyclocarbonate (CC) groups. Cyclocarbonated lignin (CC lignin) formed from this protocol was cured with diaminododecane only to form materials too brittle for mechanical characterization.<sup>26</sup> A final report for a NIPU was submitted for liginosulfuric acid that did use organic carbonates in the cyclocarbonation reaction, yet no mechanical testing was performed.<sup>27</sup>

An additional difficulty arising out of NIPU synthesis is the ability to process these materials into foams. Previous NIPU foams have used the addition of physical or chemical blowing agents such as supercritical CO<sub>2</sub>,<sup>28</sup> sodium bicarbonate<sup>29</sup> (physical) or poly(methylhydrosiloxane) (PMHS, chemical).<sup>30,31</sup> The properties of the foams produced in these reports typically show high density rigid foams between 100-300 kg/m<sup>3</sup> with little mechanical testing of compressive strength or modulus. An important characteristic of commercial rigid foams is the 10% compression strength benchmark of 100 kPa.<sup>32</sup>

The motivation behind the current work is to overcome the many challenges associated with using lignin to create a NIPU foam meeting properties commensurate with

commercial materials while utilizing non-toxic and benign reagents. To maximize the relevance of the protocol, industrial Kraft lignin was used without fractionation or depolymerization as the lignin source and non-toxic organic carbonates were employed to functionalize NIPU precursors. A fatty-acid based diamine composed of 100% biobased carbon incorporated soft-segments throughout the NIPU structure during the curing reaction. Most importantly, the functionalization with organic carbonates enabled a fast gelation reaction with the biobased diamine curing on timescales equivalent to the foaming reaction. The study presented here is the first to elucidate a pathway towards producing lignin-based NIPU foams that overcome both the reactivity and solubility constraints that often hamper lignin's wider application. The materials that have resulted represent a significant step forward in a sustainable approach to lignin-based polyurethane synthesis.

## **Experimental**

### **Materials**

Kraft lignin for this study was supplied by Domtar (Fort Mill, SC, USA) under the trade name "BioChoice Lignin". Biochoice is a low ash content (~1%) softwood Kraft lignin and was dried before use. The phenolic content of the Kraft lignin is present in Table S1. The curing agent was kindly provided by Croda International Plc (East Yorkshire, United Kingdom) under the trade name "Priamine 1074". Priamine is a dimer diamine with amine value of 209 mg KOH/g. Glycerol carbonate (GC) was purchased from Spectrum Chemical (New Brunswick, NJ, USA) or InKemia Green Chemicals (Houston, TX, USA) with a minimum purity of 90%. Dimethyl carbonate (DMC, > 99.0%),

dimethylsulfoxide-*d*6 (DMSO-*d*6, 99.96 atom% *D*), 1,8-diazabicyclo[5.4.0]undec-7-ene (DBU, 98%), 1,5,7-triazabicyclo[4.4.0]dec-5-ene (TBD, 98%), 2-chloro-4,4,5,5-tetramethyl-1,3,2-dioxaphospholane (95%), 1,3,5-trioxane (>99%), cholesterol (>99%), chromium(III) acetylacetonate (97%) and poly(methylhydrosiloxane) (PMHS) was purchased from Millipore Sigma (St. Louis, MO, USA). DMSO (99%) for reactions was purchased from VWR (Radnor, PA, USA).

### **Step One: Oxyalkylation**

Kraft lignin (6.1 mmol/g OH measured by  $^{31}\text{P}$  NMR) was mixed in a round bottom flask with 10 equivalents of glycerol carbonate (GC) (MW = 118.09 g/mol) according to the hydroxyl content of lignin. The catalyst was added in 0.1 equivalents and the reaction was conducted under a nitrogen atmosphere at 150°C for 1.5 hours. When the reaction was completed the mixture was allowed to return to room temperature and the product was precipitated in a dilute HCl solution until the pH reached a value below 2. The precipitated lignin product was washed with acidified water, filtered, and dried under vacuum over  $\text{P}_2\text{O}_5$  overnight. Typical yields of oxyalkylated lignin (OKL) resulted in a 10% increase in mass based on the addition of GC to the initial mass of Kraft lignin. The yield is influenced by lignin condensation reactions (lowering the overall hydroxyl content) and fractionation of the lignin backbone (decreasing molecular weight) making calculations of the theoretical yield difficult (see Table S1).

### **Step Two: Cyclocarbonation**

Oxyalkylated Kraft lignin (4.7 mmol/g OH, measured by  $^{31}\text{P}$  NMR ) was dissolved in DMSO and 5 equivalents of dimethyl carbonate (DMC) was added



according to the hydroxyl content of OKL along with 0.4 equivalents of the catalyst,  $K_2CO_3$ . The reaction was completed for 4 hours under nitrogen at  $75^\circ C$ . After the reaction was completed, the product was precipitated, filtered, and dried in a similar manner as step one. Typical yields of cyclocarbonated lignin (CC lignin) after the ring-closing trans-esterification reaction was 96-98% based on the initial mass of OKL.

### **Step Three: Polymerization**

CC lignin (2.0 mmol/g cyclocarbonate, measured by  $^{13}C$  NMR) was dissolved in DMSO in a 20 ml scintillation vial. The dimer diamine (MW = 537 g/mol, functionality = 2) was added according to different stoichiometric ratios of the CC groups to amine functionality (CC : amine 1:1, 1:1.5, 1:2). DMSO was added according to the following ratio: 1.3 mL DMSO : 1g CC lignin. The reaction mixture heated gently to allow the dissolution and mixture of both components and then poured in preheated molds at and subjected to curing at  $80^\circ C$  for 4 hr.,  $150^\circ C$  for 4 hr., and  $80^\circ C$  for 2 hr.

### **Foam Processing**

1 gram of CC lignin was dissolved in 1.3 mL DMSO in a 20mL scintillation vial. The dimer diamine was added according to a 1:1 and 1:2 ratio of CC: amine groups based on the molar mass of the diamine and its density (0.9 g/mL). PMHS was added based on a 1.5 and 3.0% volume fraction of the total reaction mixture. A corresponding amount of diamine was added based on a 90% mass content of the hydrosiloxane unit in PMHS.<sup>30</sup> The mixture was stirred for 1 minute and added to conical aluminum molds with a base diameter of 30 mm. Foams were subjected to curing at  $150^\circ C$  for 12 hours. When finished, the product was cut to 25 x 25mm square sections and subjected to compression testing.

## Characterization

### Chemical Analysis

Infrared spectra were collected by a Thermo Nicolet 6700 spectrometer (ThermoFischer Scientific, Waltham, MA, USA) from 500 – 4500  $\text{cm}^{-1}$  using 16 scans with a 2  $\text{cm}^{-1}$  spectral resolution. All NMR experiments were completed by a Bruker Avance 300 MHz spectrometer (Billerica, MA, USA).  $^1\text{H}$  NMR was taken after dissolving 30 mg of lignin samples in 0.55 ml of DMSO-*d*6. 32 scans were completed using a spectral width of 5342 Hz.  $^{13}\text{C}$  NMR was completed by dissolving 70-80 mg of lignin samples in 0.55 ml of DMSO-*d*6 with 50  $\mu\text{L}$  of a 15 mg/mL solution of trioxane as internal standard. Chromium(III) acetylacetonate was used as relaxation agent with a spectral window of 18,110 Hz and 20,000 scans.  $^{31}\text{P}$  NMR analysis was completed using 2-chloro-4,4,5,5-tetramethyl-1,3,2-dioxaphospholane as phosphorylating agent in a 1.6/1 solution of pyridine and chloroform-*d* according to established procedures.<sup>33</sup> Cholesterol was used as an internal standard and Cr(III) as relaxation agent. CP/MAS SS  $^{13}\text{C}$  NMR was conducted using a Bruker AV3-400 instrument with a spectrometer frequency of 100 MHz and a magical angle spinning frequency of 10 kHz. The molecular weight of lignin precursors was measured using an Alliance GPCV 2000 (Waters, Millford, MA, USA) with two columns used in series: first a Waters Styragel® HT5 followed by an Agilent PolarGel-L column. Lignin was dissolved in *N,N*-dimethylformamide at 1 mg/ml in 0.05 lithium bromide. The mobile phase was filtered using a 0.2 mm nylon filter. PEG calibration standards were used in tandem with a Waters differential refractometer. Lignin samples were detected by a Waters 2487 UV-Vis detector at 280 nm. Biobased content was

completed by Beta Analytic testing laboratory (Miami, FL, USA) according to ASTM D6866 to determine the percent Modern Carbon (pMC) and biobased content.

### **Mechanical Analysis**

Tensile testing was completed on dog bone shaped samples created in silicon molds and tested on an Instron 1125R (Norwood, MA, USA) with a 1 kN load cell at 5 mm/min. Compression testing was completed on an Instron 5582 with 1 kN load cell at a compression rate of 10 mm/min. Samples were cut from conical molds to cubes of approximate dimensions of 25mm x 25mm x 10mm (depending on rise height). Modulus was calculated for both tensile and compression samples based on the initial slope of the stress-strain graph. Three to five samples for tensile testing and five samples for compression testing were averaged and used for statistical analysis with error reported as the standard deviation. Dynamic mechanical analysis was completed on a TA Instruments (New Castle, DE, USA) DMA Q800 using a fiber/film tension clamp under single cantilever mode. A temperature sweep was analyzed from -50°C to 150°C at a frequency of 5 Hz and 0.3% max strain.

### **Thermal Analysis**

Thermogravimetric analysis (TGA) was completed on a TA Instruments Q5000 using a 20°C/min heating rate from 25°C to 600°C under a mixture of nitrogen and air. Dynamic Scanning Calorimetry was completed on a TA Instruments Q20 during a heat-cool-heat cycle at 10°C/ min with 50mm/min nitrogen purge. The glass transition temperature was calculated based on the midpoint of the change in slope of heat flow vs. temperature. Curing rheology was studied on a Discovery HR-2 rheometer (TA

Instruments) using a 25 mm parallel plate geometry. The rise in loss and storage moduli were observed using a time sweep under isothermal condition at 80°C, 1% strain and an angular frequency of 10 rad/sec.

## **Results and discussion**

### **Step One: Oxyalkylation of Kraft Lignin**

The first step in the synthetic scheme employed non-toxic glycerol carbonate (GC) to act as solvent and reagent in the oxyalkylation of unmodified Kraft lignin. The aliphatic and aromatic hydroxyls of lignin were utilized to react with GC and incorporate liable ether and carbonyl groups on the backbone of lignin while terminating the chain extended precursor in a 1,2-diol (Figure 1). In a subsequent step, this 1,2-diol functionalized structure will undergo a transesterification reaction with dimethyl carbonate (DMC) to insert 5-member cyclocarbonate structures on the lignin backbone<sup>19</sup>. The reaction of lignin derived OH groups with organic carbonates has been shown in previous reports to react at both the carbonyl and alkyl carbons forming carbonate and ether linkages, respectively. Kuhnel et al. found with organosolv lignin and propylene carbonate that an almost exclusive reaction was found at the alkyl carbons creating ether linkages at temperatures above 170°C.<sup>12</sup> However, other groups have found at lower temperatures (90-150°C) that both carbonate and ether linkages are present after the reaction of lignin with organic carbonates.<sup>14,15</sup>

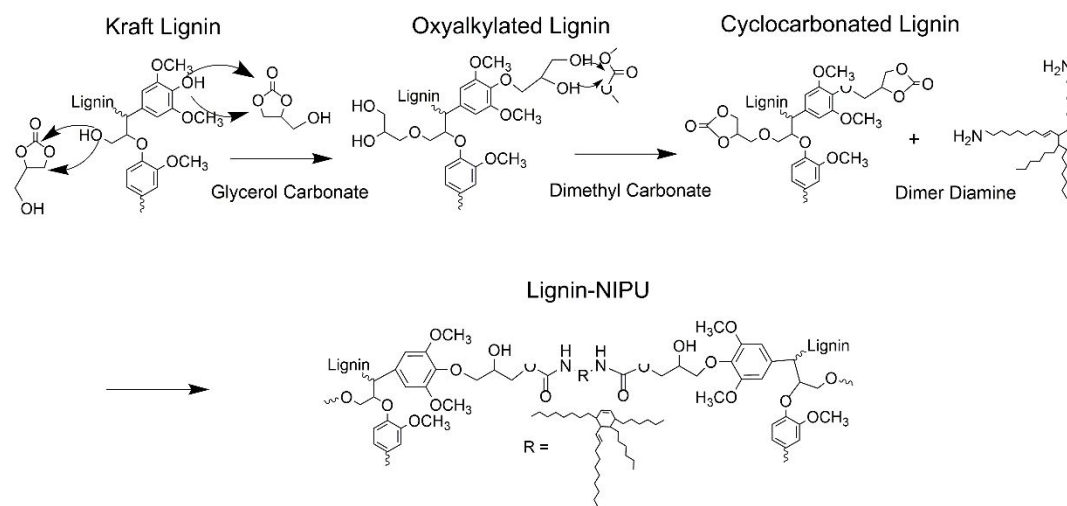


**Figure 1:** Reaction diagram for the functionalization of Kraft lignin with cyclic carbonates and curing with a fatty acid-based diamine.

The spectroscopic evidence presented here (Figure S1 and S2) supports the incorporation of chain extended lignin macromers containing both types of liable groups, creating unique molecular handles that could be used in the chemical recycling of polymers at a later time.

The lignin used for this study is Biochoice Kraft lignin (KL) from Domtar containing the hydroxyl content seen in Table S1. The overall hydroxyl content of the raw Kraft lignin and that functionalized with organic carbonates was measured using quantitative <sup>31</sup>P NMR according to established techniques.<sup>33</sup> Briefly, lignin was dissolved in a suitable solvent and a phosphorylating agent was added to react with the aliphatic and

aromatic hydroxyl units. The signal for these hydroxyl units can be measured by  $^{31}\text{P}$  NMR and compared to an internal standard to quantitatively measure the hydroxyl content of lignin. The total hydroxyl content of lignin was used to measure reactive equivalents of GC and DMC in the functionalization of lignin with cyclocarbonates. The oxyalkylation of lignin with organic carbonates has been studied in the past showing an intense sensitivity to reaction time, temperature, and catalyst loading.<sup>11-14</sup> Initial reactions using 10 equivalents of GC, 0.1 equivalents of the catalyst DBU at 170°C for 3 hours often produced dark, glassy materials characteristic of polycarbonate condensation between KL and GC. A similar result was observed by Liu et al. in their preparation of oxyalkylated derivatives using ethylene carbonate.<sup>10</sup> Lowering the temperature to 150° while keeping reaction time the same still resulted in material showing substantial insolubility and unable to process. However, reducing the reaction time to 1.5 hour and lessening the catalyst loading to .05 equivalents produced a product completely soluble in DMSO and capable of characterization and further synthetic efforts. We therefore observed that the reaction of GC with Kraft lignin was highly temperature sensitive. It is well known that at temperatures near Kraft pulping conditions (170°C) the ether bond linkages throughout lignin's structure can be broken setting in motion a cascade of reactions involving highly reactive lignin fragments<sup>34</sup>. Under higher catalyst loadings and longer reaction times an increase in evolved gas ( $\text{CO}_2$ ) was observed pointing to the reaction of additional GC on the backbone of lignin. Recovery of lignin after such reactions became increasingly difficulty as the lignin polyol had a much higher solubility in the aqueous media.

The evidence of a complete reaction of aromatic hydroxyls with GC can be followed by  $^{31}\text{P}$  NMR through the disappearance of the aromatic signal from 136-144 ppm (Figure 2). New peaks appear in the aliphatic region from 145.5-146.5 ppm corresponding to the conversion of aromatic hydroxyls to newly formed aliphatic hydroxyl groups. Interestingly, when the reaction is completed at  $120^\circ\text{C}$ , evidence of an incomplete reaction is seen by the persistence of aromatic hydroxyl groups between 137-140 ppm. Table S1 shows that the molecular weight of OKL slightly decreases from unfunctionalized Kraft lignin with a corresponding decrease in hydroxyl content. The condensation of lignin structures (lowering the hydroxyl content) as well as the fractionation of the lignin backbone (leading to lower molecular weight derivatives) has been observed in other reports and is a result of the temperature and catalyst loading used in functionalization techniques.<sup>11,14</sup> In addition to the reaction of the aromatic hydroxyl groups, the conversion of native aliphatic hydroxyl groups can be seen by new, sharp peaks formed in the aliphatic region between 147-148 ppm (Figure 2:  $^{31}\text{P}$  NMR of ). Given the evidence of the successful functionalization of aliphatic and aromatic hydroxyl groups, as well as the solubility of the sample processed at  $150^\circ\text{C}$  for 1.5 hr., these conditions were used for all subsequent synthetic efforts.

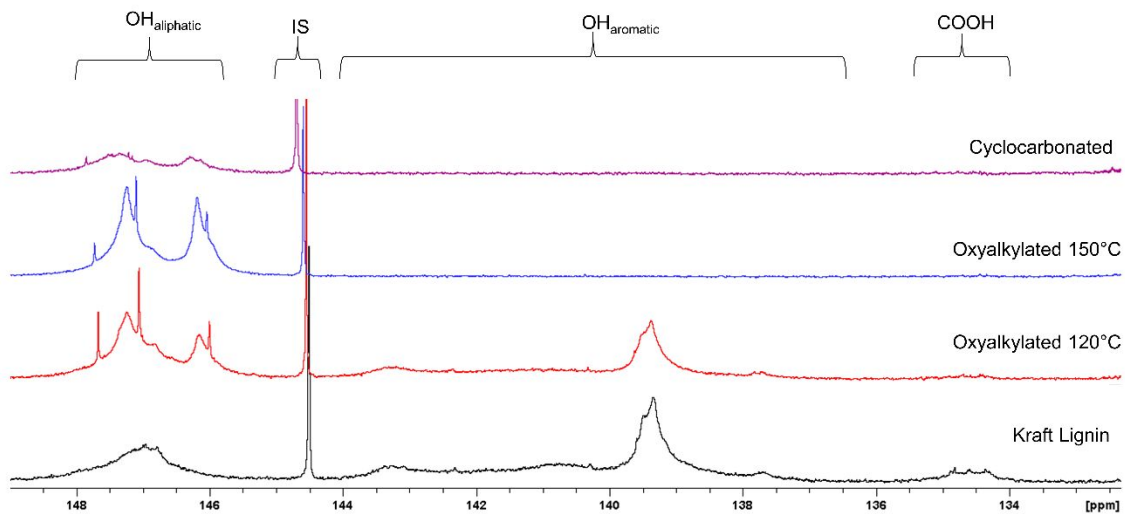


**Figure 2:**  $^{31}\text{P}$  NMR of Kraft lignin and functionalized products. The disappearance of the phenolic hydroxyl peaks from 134-144 gives evidence to a complete conversion of these groups to aliphatic hydroxyl groups after the reaction with GC.

$^1\text{H}$  NMR also confirms the successful insertion of oxyalkylated chains with a sharp peak appearing at 3.7 ppm associated with the alkyl protons of the newly grafted carbon chains and the disappearance of the phenolic protons from 8-10 ppm in the unfunctionalized lignin (Figure S1). Signals appear in the region for cyclocarbonate protons (4-5 ppm) even during the first stage with GC, a phenomena observed by other groups and most likely a result of a transesterification reaction with excess GC in the reaction mixture.<sup>14,19</sup> Since the newly formed peaks for the oxyalklyated chains overlap with existing signal from unreacted lignin, quantification is difficult. However, integrating the total signal from all hydrogen associated with the methylene and methoxy region present between 3.5 to 4.5 ppm in Figure S1 and comparing this result to the aromatic signal present from 8 to 10 ppm, an average of 12 additional hydrogen atoms were added



per aromatic group. When this number is compared to the amount of hydrogen contained in each grafted strand of GC (5) a reasonable correlation with 2 grafted glycerol chains per aromatic unit can be made. This result supports the findings by other groups that the reaction of lignin with organic carbonates is controlled to the extent that extended polyglycerol chains are not formed under normal reaction conditions. For example, Kuhnel et al. found with extensive  $^{13}\text{C}$  analysis that approximately 2.1 to 2.5 alkyl strands were grafted when GC was used with Kraft lignin.<sup>13</sup> In our analysis,  $^{13}\text{C}$  NMR did not provide high enough resolution to make a more quantitative study of the amount of alkyl chains added to the lignin structure. The difficulty of quantifying the amount of grafted chains is shared by other groups, e.g., Duval et al. in their work with organic carbonates and Soda lignin.<sup>14</sup>

The FTIR spectra of oxyalkylated Kraft lignin shows the successful grafting of oxyalkylated strands with an increase in signals in the 1100 - 1200  $\text{cm}^{-1}$  region associated with C-O stretching as well as an increase in the overall O-H signal at 3500  $\text{cm}^{-1}$  as a result of the O-H terminated groups (Fig. S2). The carbonyl region of the oxyalkylated precursor shows an interesting result. The side peak at  $\sim 1725$   $\text{cm}^{-1}$  shows the formation of carbonyl groups witnessing to the formation of linear carbonate linkages between lignin hydroxyl groups and GC. Cyclocarbonate groups (CC) can also be found after the reaction with GC as witnessed by the peak at 1795  $\text{cm}^{-1}$ . Overall, the FTIR spectrum confirms the presence of both etherified and carboxylated groups in the oxyalkylated strands successfully functionalizing lignin with extended hydroxyl groups utilized in a second step for cyclocarbonation.

### Step Two: Cyclocarbonation of Lignin

The diols present on the lignin structure are converted to cyclocarbonate groups by a subsequent reaction with dimethyl carbonate (Figure 1). The successful reaction is confirmed by the increase in the CC peak at  $1795\text{ cm}^{-1}$  in FTIR (Figure S2) as well as the increase in prominence of the hydrogens associated with the carbonate ring at 4.5-5.5 ppm in the  $^1\text{H}$  NMR (Figure S1). Quantification of the CC groups was made through the application of  $^{13}\text{C}$  NMR by comparing the characteristic peak of the cyclocarbonate at 155 ppm to that of an internal standard (trioxane) at 90 ppm (Figure ). Quantification showed a lignin derivative containing a concentration of CC groups of  $2.05 \pm 0.05\text{ mmol/g}$  lignin. This result is slightly higher than that found for Organosolv lignin by Kuhnel et al. ( $1.5\text{ mmol/g}$ )<sup>19</sup> who originally reported on the transesterification approach and very similar with Salanti et al.<sup>25</sup> who used the  $\text{CO}_2$  insertion approach on Kraft lignin ( $2.01\text{ mmol/g}$ ).

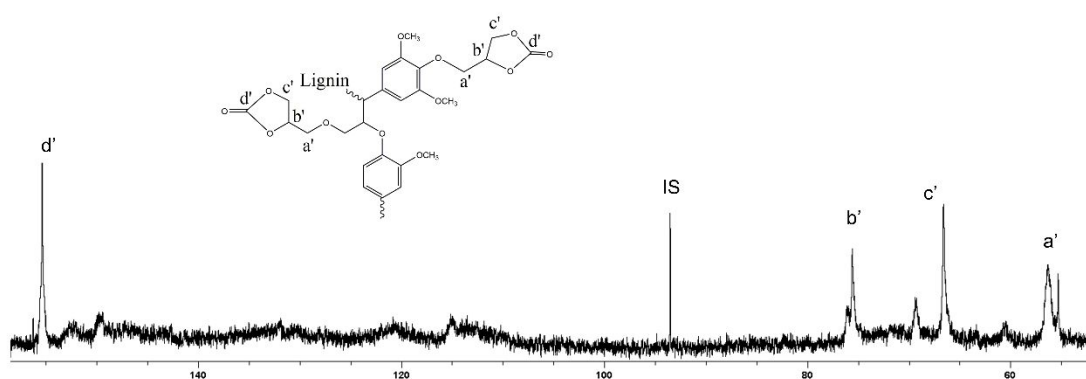


**Figure 3:**  $^{13}\text{C}$  NMR of CC lignin. The peak associated with cyclocarbonate groups at 155 ppm was compared to the internal standard trioxane to calculate the concentration of CC groups per gram of lignin.

## NIPU Synthesis

The final step in this synthetic scheme involved the addition of a fatty acid-based dimer diamine as curing agent containing 100% renewable carbon. The proprietary diamine is not given a molar mass by the supplier but does contain a reported amine value of 209 mg KOH/g. Using equation 1 and the amine value,<sup>30</sup> it is possible to calculate the molecular weight of the diamine as 537 g/mol in good agreement with previous reports using Priamine.<sup>35</sup>

$$MW = 56,100 \times (\# \text{ of amine H's}) \div (\text{amine value} \times \# \text{ of H's per N}) \quad (1)$$

Dimer diamines from fatty acids have been used in the past to synthesize NIPU materials from sebacic biscyclocarbonate,<sup>35,36</sup> carbonated soybean oil,<sup>37</sup> or from other carbonated vegetable oils.<sup>38</sup> The aliphatic nature of the carbon chain present in the structure of the dimer diamine provides soft segments to the NIPU structure and is utilized in this study to temper the brittle and rigid nature of the lignin aromatic backbone. NIPU materials were formed by mixing CC lignin with different stoichiometric ratios of the diamine (CC : amine - 1:1, 1:1.5, 1:2) to study to difference in crosslinking density and mechanical properties afforded by the different reaction mixtures. A stoichiometric amount of diamine theoretically leads to the highest amount of crosslinking while excess diamine terminates the crosslinking reaction by creating amine-terminated lignin derivatives<sup>39</sup> (Figure S3). A small amount of DMSO was used to aid in dissolution and compatibilization of the two constituents and the organocatalyst TBD was used at 0.1

equivalents to ensure a full reaction between CC groups and amines. It must be noted that part of the innovation of this approach is the synthesis of CC precursors that can be compatibilized with a biobased curing agent. The reaction conditions presented above were tailored to produce a functionalized lignin molecule of small enough molecular weight that allowed easy compatibilization with the fatty acid-based diamine. This protocol stands as a significantly more environmentally friendly approach to produce soluble lignin precursors as compared to dissolution in polyhydric alcohols<sup>26,40,41</sup> or PO, significantly reducing the bio-content of cured materials, or the use of chlorinated and toxic solvents such as dichloromethane<sup>42,43</sup> and tetrahydrofuran.<sup>24,26,10</sup>

The kinetics of the curing reaction was studied by monitoring the gel time of the reaction mixture at 80°C using a parallel plate rheometer (Figure 4). The gel time of a polyurethane is a very important aspect of its processability and the ability to cure on time-scales commensurate with foaming reactions. Rheology can indicate the gel time of a polymer by monitoring a sharp increase in the elastic modulus as well as the crossover point between elastic and storage moduli referring to the point where the reaction mixture takes on solid rather than liquid mechanical characteristics. The results of the rheology study are seen in Figure 4 showing that a sharp increase in elastic modulus for the uncatalyzed sample at around 6.5 minutes and that for the catalyzed system around 1.5 minutes. Given that a time of 1.5 minutes was needed to lower the geometry of the rheology instrument and start the program, the gel time of the uncatalyzed system stands at 8 minutes and that of the catalyzed system at 3 minutes. Fast gelation times such as these are surprising given that one of the main difficulties found for NIPU materials is the

low reactivity between cyclocarbonates and diamines leading to extended gel times.<sup>44</sup> The fast reaction time of the current NIPU system gives evidence to the successful ability of using organic carbonates as benign reagents to make more reactive lignin precursors. If the reaction of Kraft lignin with GC was not able to extend the nascent hydroxyl groups beyond the complicated structure of the lignin backbone, the cyclocarbonate groups would remain sterically hindered from participating in the curing reaction. The fast kinetics observed here demonstrate the creation of a highly reactive lignin precursor using a non-toxic protocol.

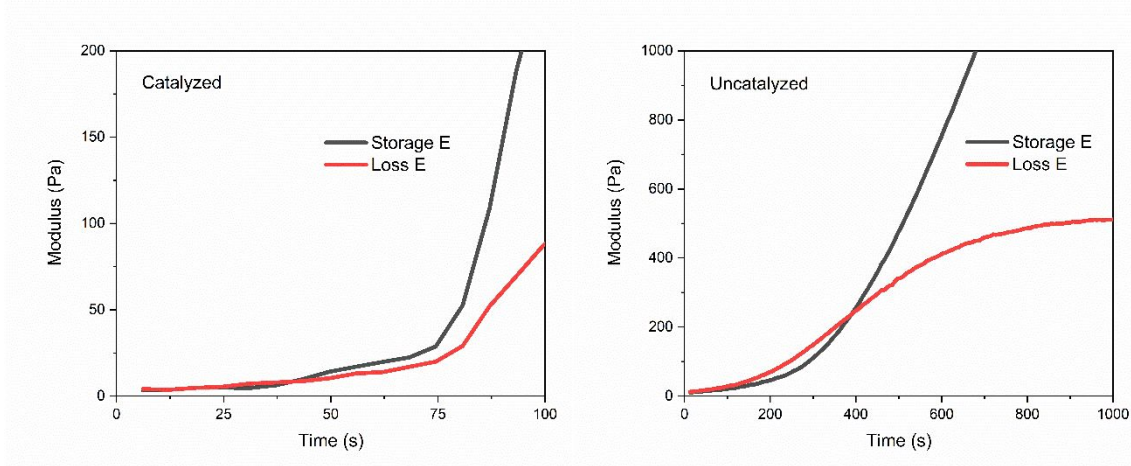


**Figure 4:** Curing rheology of the NIPU reaction mixture. A sharp rise in the elastic modulus demonstrates the beginning of the gelation point in the reaction of cyclocarbonated lignin and the diamine curing agent.

Due to the heavily crosslinked nature of the NIPUs and the increase in hydrogen bonding created from the extra hydroxyl group formed during the ring opening reaction during curing,<sup>35</sup> the synthesized material showed complete insolubility in common organic solvents as well as treatment with hexafluoroisopropanol and trifluoroacetic anhydride. For this reason, the extent of the polymerization reaction was monitored by FTIR watching the

conversion of the CC peak at  $1795\text{ cm}^{-1}$  to the C-N-O stretch of the urethane carbonyl at  $1720\text{ cm}^{-1}$ . Figure 5A shows the FTIR of NIPU samples cured with increasing temperature. The sample cured at  $80^\circ\text{C}$  still shows unreacted cyclocarbonate groups present in the structure whereas increasing the curing temperature to  $110^\circ\text{C}$  shows a smaller proportion of unreacted groups. When the curing temperature is increased to  $150^\circ\text{C}$  the complete conversion of cyclocarbonate groups to urethane groups is observed. Therefore, the maximum curing temperature of  $150^\circ\text{C}$  was chosen for the curing reaction.

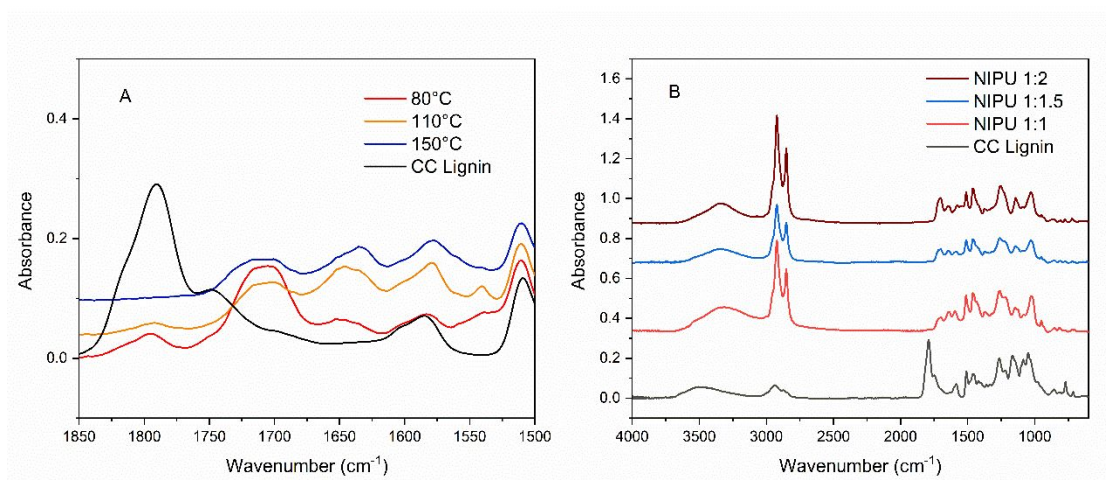


**Figure 5:** FTIR of cured NIPU materials. A) Expanded view of the carbonyl region of materials cured at different temperatures. B) FTIR of different reaction stoichiometries compared to CC lignin.

The complete reaction of cyclocarbonate groups is an important reaction parameter to synthesize high performing NIPU materials. Having found the successful conditions leading to the conversion of cyclocarbonate groups to urethane bonds, a series of samples varying the stoichiometry of the curing agent were made. Samples were synthesized using a ratio of CC lignin: amine of 1:1, 1:1.5, and 1:2. FTIR shows that all NIPU samples observe a complete conversion of the cyclocarbonate peak at  $1795\text{ cm}^{-1}$  to urethane

carbonyls at  $1720\text{ cm}^{-1}$  as well as a side peak at  $1640\text{ cm}^{-1}$  showing the existence of urea groups within the structure (Figure 5B and S4). Urea groups occur at high curing temperatures when unreacted amine groups attack newly formed carbonyl groups forming rigid N-C-N bonds. The presence of urea groups is not surprising at a cure temperature of  $150^\circ\text{C}$  and is also common in conventional polyurethanes formed through the reaction of diisocyanates.<sup>45</sup> The large peaks at  $1600\text{ cm}^{-1}$  and  $1500\text{ cm}^{-1}$  are caused by the aromatic skeletal bands of lignin and hide the N-H deformation normally found around  $1500\text{ cm}^{-1}$ .<sup>46</sup> The incorporation of the aliphatic diamine is witnessed by the replacement of the OH stretch at  $3500\text{ cm}^{-1}$  in the cyclocarbonated lignin precursor to the N-H stretch at  $3300\text{ cm}^{-1}$  as well as the large increase in the methylene signal present as two peaks centered around  $2900\text{ cm}^{-1}$ .<sup>47</sup>

To further probe the chemical structure of the synthesized NIPUs, solid state (ss) NMR was utilized given the insolubility of the materials in common solvents used to prepare conventional NMR. SS NMR provided excellent structural characterization of NIPU 1:1 and NIPU 1:2 compared to the CC lignin precursor (Figure 6). Structural assignment was made based on literature reports.<sup>26,48</sup> The reaction of CC lignin with the aliphatic dimer diamine showed a shift in the cyclocarbonate carbonyl present at 155 ppm (d) to a urethane bonded carbonyl slightly downfield (d'). In the alpha position to the urethane bond is an aliphatic C-N bond which appears at 40 ppm when the diamine is crosslinked and 39 ppm when the diamine is a chain terminating species ("free"). NIPU 1:2 shows a higher signal for "free" C-N bonds than NIPU 1:1 as the excess curing agent limits the amount of crosslinking available during the reaction by creating amine

terminated lignin species. The signals for the cyclocarbonate carbons a-c in CC lignin become condensed after the curing reaction showing the more similar chemical environment for C-O and C-O-H (a'-c') carbons after the curing reaction. Farther upfield the methylene signal appears at 30 ppm reflecting the incorporation of the long-chained dimer diamine. The signal in this region for NIPU 1:2 is larger than NIPU 1:1 reflecting the larger amount of the curing agent added in the reaction mixture. Overall, ss NMR confirms the successful reaction of CC lignin and the curing agent as well as pointing out the relevant structural features that accompany an increase in the aliphatic curing agent.

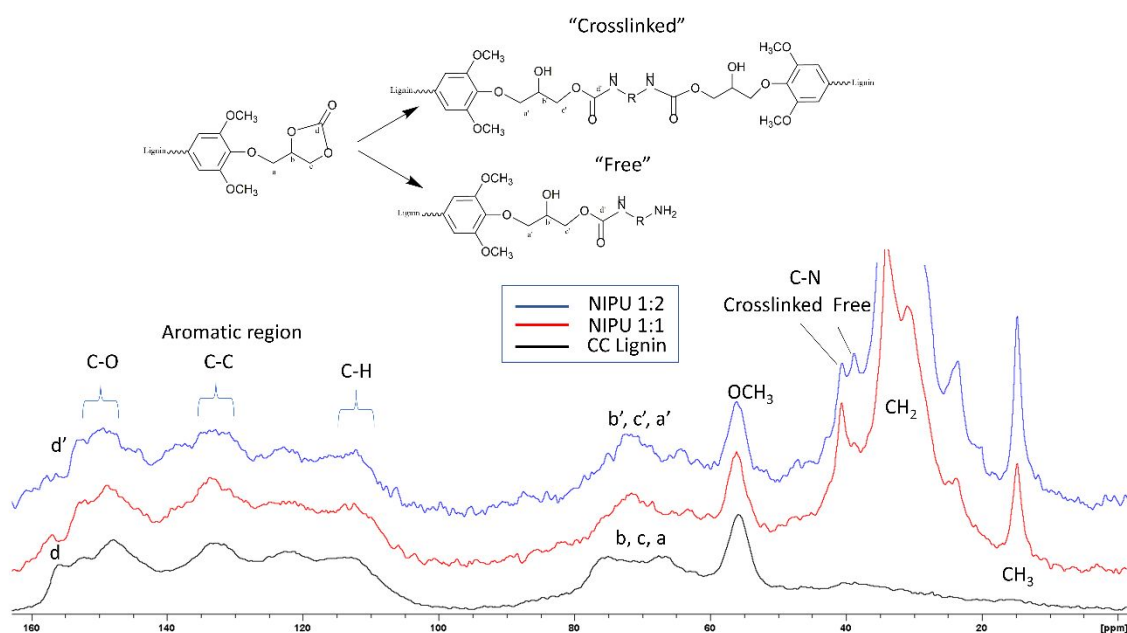


**Figure 6:** Solid state NMR of NIPU 1:1 and NIPU 1:2 compared to CC lignin

### Thermal and Mechanical Properties

Tensile tests were completed on dog bone shaped samples using a 1 kN load cell and 5 mm/min crosshead speed. Samples using a curing agent ratio of 1:1, 1:1.5 and 1:2



(CC lignin : amine) were tested to explore the change in mechanical properties as the crosslinking density is changed. The results reported in Table 1 show that the highest average ultimate strength values of 20.9 MPa are obtained when a stoichiometric ratio is used (1:1) between CC lignin and diamine. The stoichiometric samples did demonstrate some difficulty when clamping during tensile testing. However, adding a slight excess (no more than .25 mol fraction) of the diamine before curing allowed for less cracking during analysis with no observable difference in tensile strengths. Higher ratios of diamine (NIPU 1:1.5 and 1:2) incorporate larger proportions of fatty acid-based soft segments in the polymeric structure leading to an increase in the strain-at-break values and a corresponding decrease in modulus. When the ratio of amine groups to CC groups is increased to 2 (NIPU 1:2) a dramatic increase in the ultimate strain and decrease in modulus is observed pointing to more flexible samples. The NIPU 1:2 sample represents the highest theoretical amount of soft segment incorporation in the polymeric structure by inserting a long-chained diamine molecule at each CC group (Figure 6 and S3). The decrease in ultimate tensile strength and modulus is complimented by the results of DMA analysis showing a decrease in crosslinking density of NIPU 1:2 in DMA presented below. Overall, the tensile test results confirm the molecular structure determination of ss NMR that revealed a higher incorporation of soft segments (aliphatic diamine) in the NIPU 1:2 sample leading to a dramatic increase in the elasticity of these materials. Representative stress-strain curves for each sample is presented in Figure 7.

**Table 1:** Uniaxial tensile testing results for different NIPU formulations.

NIPU	Ultimate Tensile	Ultimate Strain	Tensile Modulus
------	------------------	-----------------	-----------------

	Strength (MPa)	(%)	(MPa)
1:1	$20.9 \pm 3.6$	$10.7 \pm 2.8$	$400.6 \pm 86.0$
1:1.5	$15.8 \pm 2.2$	$13.0 \pm 4.0$	$307.7 \pm 45.3$
1:2	$12.2 \pm 0.54$	$38.9 \pm 7.5$	$137.3 \pm 23.8$

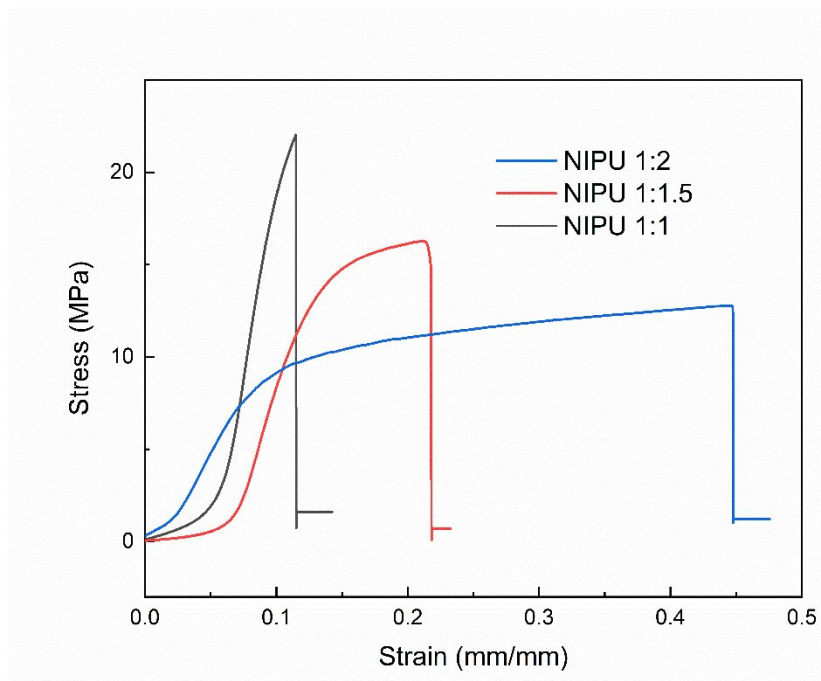


**Figure 7:** Uniaxial tensile testing of different NIPU formulations. Higher incorporations of the fatty-acid based diamine increases the elasticity of samples through larger soft-segment distributions.

These results stand, to the best of our knowledge, as the highest mechanical properties gained for a lignin-derived NIPU. In addition, these results meet and exceed studies with diisocyanate-based lignin polyurethanes using fatty-acid based functionalization measures. Laurichesse et al. used oleic acid functionalized lignin to synthesize conventional diisocyanate PUs finding ultimate strength values as high as 9.6 MPa for a 63% biobased polymer.<sup>49</sup> Tavares et al. used castor oil with Kraft lignin to reach tensile stress values as high as 23.5 MPa for a 30% lignin-based diisocyanate PU.<sup>50</sup> Given the range of tensile strengths typically encountered for commercial PUs (1.7 – 40 MPa),<sup>50</sup> these materials

present an attractive material with enhanced sustainability. However, relatively large standard deviations were observed for the stress / strain values of each material. This result is not surprising given the large PDI reported for the CC lignin precursors (Table S1: PDI = 4.1) and the known heterogeneity of lignin from sample to sample.<sup>2</sup> Indeed, many research efforts have endeavored to convert lignin to a more homogeneous precursor material through a variety of fractionation, depolymerization and chemical conversion technologies.<sup>1</sup> This study exists to demonstrate the ability to use an industrial technical lignin to produce materials of high value.

Thermal analysis of the NIPUs showed a material with similar thermal stability to commercial polyurethanes. TGA analysis (Figure S5) revealed 5% weight loss temperatures ( $T_{5\%}$ ) above 300°C, much higher than typical values of NIPUs at 250°C.<sup>36</sup> Thermal breakdown followed a typical two-step mechanism as revealed by the curve for the first derivative of weight loss (Figure S5). The first derivative shows the dissociation of the urethane and lignin components around 350°C followed by rapid breakdown of the diamine constituents.

DSC results showed no peaks for melting or crystallizing events in the temperature range from -20°C to 200°C typical of thermosetting crosslinked materials (Figure S6). Glass transition temperatures were measured from the change in slope present in the second heating curve of DSC thermograms. As expected, higher loadings of the aliphatic curing agent created a more dramatic transition from the glassy state while  $T_g$  decreased from 94°C in NIPU 1:1 to 84°C in NIPU 1:2. These results aligned well with the glass transition temperature found from DMA analysis. DMA was completed at a fixed frequency (5 Hz)

from -50°C to 150°C showing properties of a crosslinked material. The peak in the Tan Delta plot is associated with the  $T_g$  of the polymer network (alpha relaxation) and is observed to decrease from 99°C with NIPU 1:1 to 91°C for the 1:2 NIPU sample (Figure S7). The alpha relaxation found in NIPU 1:2 is much broader and results from the relaxation associated with the dimer diamine while that at higher temperature is associated with the lignin macromolecular structure.<sup>51</sup> The plots for DMA thus reflect a dual-phase material with a broad transition region between 0°C and 100°C. The existence of a dual phase polymer structure enables the exploration of the shape memory effect described below.

Using viscoelastic polymer theory, it is possible to measure the crosslinking density and molecular weight between crosslinks using the rubbery plateau found in the storage modulus after the alpha relaxation temperature in DMA.<sup>30</sup> The rubbery plateau can be found at  $T_{\alpha+20}$  located after the broad transition from the glassy region. (Figure S7). The crosslinking density ( $V_e$ ) can be found through equation 2:

$$V_e = \frac{E'}{3RT} \quad (2)$$

where  $E'$  is the elastic modulus at  $T_{\alpha+20}$ ,  $R$  is the gas law constant and  $T$  is  $T_{\alpha+20}$ . The crosslinking density for each samples is displayed in Table 3 and is seen to decrease with increasing soft segment incorporation from NIPU 1:1 to NIPU 1:2. A high degree of crosslinking is observed creating exceptionally high storage modulus ( $\sim 14$ - $20$  MPa) in the area of the rubbery plateau.

The average molecular weight of crosslinks ( $M_c$ ) can be found by using the data from the rubbery plateau and equation 3:

$$M_c = \frac{3\rho RT}{E'} \quad (3)$$

where  $\rho$  is the density of the polymer,  $T$  is  $T_{\alpha+20}$  and  $E'$  is the elastic modulus at  $T_{\alpha+20}$ . Using this relationship, the average molecular weight between crosslinks in the NIPU 1:1 sample was calculated to be 536.9 g/mol corresponding precisely to the molecular weight of the dimer diamine used in the curing reaction (537 g/mol). When an excess of diamine is used in NIPU 1:1.5 and NIPU 1:2, the average crosslinking molecular weight increases as a consequence of the incorporation of a larger amount of amine terminated lignin species interacting through hydrogen bonding.

**Table 2:** Thermomechanical data for NIPU samples

Sample	$T_{5\%}$	$T_g$ (DSC)	$T_{\alpha}$ (DMA)	Crosslinking Density (mol/m <sup>3</sup> )	Average MW of Crosslinks (g/mol)
--------	-----------	-------------	--------------------	--	----------------------------------

<b>1:1</b>	301°C	94°C	99.0	1863	536.9
<b>1:1.5</b>	--	---	98.2	1619	617.6
<b>1:2</b>	316°C	84.0°C	91.9°C	1538	650.2

### Shape Memory Capability

The presence of two phases in a polymer structure often results in shape memory characteristics. Shape memory polymers are desired due to their possible applications in sensors, actuators and smart materials.<sup>52</sup> Shape memory polymers typically contain hard segments responsible for the permanent morphology of the sample while soft segments allow deformation of the sample shape above the  $T_g$  of the polymer.<sup>52</sup> When the temperature is lowered below  $T_g$ , and the external stress is released, the sample retains the deformed shape due to the interaction between soft-segment polymer strands.<sup>53</sup> Given the  $T_g$  of the NIPU samples located around 100°C, the shape memory effect of the samples was tested by heating the cured NIPUs in an oven set a 105°C for 10 minutes, then inducing a semicircular deformation upon cooling at room temperature. Shown in Figure 8, the NIPU material is able to maintain the deformation after cooling to room temperature and observes reversibility back to the pre-deformed shape upon re-heating. This effect was observed for all NIPU samples regardless of the curing agent stoichiometry confirming the dual phase character of these samples and their ability to act as shape memory materials.

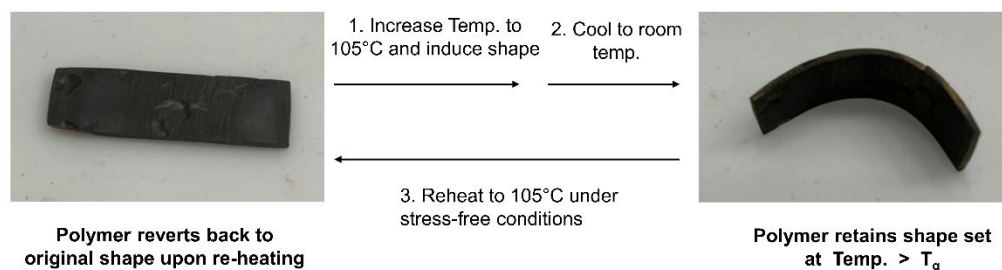


**Figure 8:** Shape memory characteristics of NIPU materials. NIPU materials-maintained deformation after heating above the glass transition temperature, applying an external stress to deform, and cooling to room temperature. The polymer reverted back to its permanent state upon a second heating cycle.

### NIPU Foams

Having verified satisfactory thermal and mechanical properties of the lignin-derived NIPU using a green protocol, a chemical foaming agent was added to the reaction mixture to study the ability to process NIPU foams. Poly(methylhydrosiloxane) was added to react with the diamine curing agent to release hydrogen gas and induce foaming. The reaction mixture viscosity of polyurethane foams is an important parameter to allow bubble coalescence during the foaming reaction increasing the porosity of the sample.<sup>54</sup> It was found through an iterative process that a ratio of 1.3 ml DMSO : 1 g CC lignin was the optimal conditions to support foam rise during the curing process. PMHS was initially added in various volume percentages relative to the reaction mixture to form the lowest density foam. It was found that at 3% PMHS volume compared to reaction mixture volume produced consistent samples with the highest rise height and lowest density. Additional diamine was added in stoichiometric proportions to react with PHMS to allow the reaction stoichiometry to remain consistent. Both the reaction mixture corresponding to the NIPU

1:1 and the NIPU 1:2 was utilized for the foaming reaction at 3% volume PMHS. Additional materials were made at 1.5% PMHS for comparison.

Table 3 shows the results for physical and mechanical testing of the NIPU foams. Low density elastomeric foams typically have values less than  $100 \text{ kg/m}^3$  and generally near  $30 \text{ kg/m}^3$ .<sup>54</sup> High density commercial rigid foams can have density values as high as  $900 \text{ kg/m}^3$ .<sup>30</sup> Densities for all formulations placed these materials in the region of high-density foams between  $241 - 337 \text{ kg/m}^3$  comparable to other reports using chemical foaming techniques.<sup>30,31</sup> A negligible difference in density is made by changing the ratio of curing agent between NIPU 1:1 and 1:2, however a noticeable difference in the properties can be seen according to the amount of foaming agent added during processing. Using a 3% amount of PMHS clearly results in lower density foams with a corresponding decrease in compressive modulus. An important property to rigid PU foams is the compressive strength at 10% strain. Commercial rigid PU foams typically meet a 100 kPa strength threshold for most applications.<sup>32</sup> Of the few reports available for NIPU foams,<sup>28-31,55</sup> no study has reported on this important characteristic. The results for compression testing in Table 4 show that this threshold has been met by the foams made from a stoichiometric amount of diamine (NIPU 1:1). Mechanical testing clearly shows using a stoichiometric amount of curing agent results in greater compressive strengths and comparable modulus to the NIPU 1:2 samples, revealing no net gains in properties using excess diamine in the 1:2 samples. The compressive testing of these foams aligns with the general principle that an increase in compressive strength is observed for materials with



higher crosslinking density (NIPU 1:1 vs. NIPU 1:2) and apparent density (1.5% PMHS vs. 3.0% PMHS).<sup>56</sup>

**Table 3:** Physical and mechanical properties of NIPU foams.

<b>NIPU / Foam %</b>	<b>Density (kg/m<sup>3</sup>)</b>	<b>Porosity <math>\phi</math></b>	<b>Volume Expansion <math>\phi</math></b>	<b>Compressive Strength (10%, kPa)</b>	<b>Compressive Modulus (MPa)</b>
1:1 / 3%	241 ± 34	0.76 ± 0.03	4.32 ± 0.60	131.8 ± 37.9	1.42 ± 0.22
1:1 / 1.5%	337 ± 57	0.67 ± 0.06	3.11 ± 0.48	170.0 ± 18.6	1.64 ± 0.32
1:2 / 3%	241 ± 45	0.76 ± 0.04	4.40 ± 0.96	79.2 ± 18.5	1.34 ± 0.25
1:2 / 1.5%	331 ± 39	0.68 ± 0.04	3.12 ± 0.37	111.9 ± 28	1.19 ± 0.30

The ability to process these lignin-based samples into foams relies upon the high reactivity established earlier between lignin-derived cyclocarbonates and the fatty acid-based diamine. The use of organic carbonates to cyclocarbonate lignin overcomes the complicated and sterically hindered structure of lignin to allow access to the diamine in the curing reaction. With a gel point found at 3 minutes for the catalyzed reaction mixture, these foams align with industrial practices that rely upon fast reaction kinetics to produce commercial polyurethane foams<sup>57</sup>.

Structural morphology of the NIPU foams was examined using SEM analysis. Figure 9 shows images of the lowest density foams at 3% PMHS. The NIPU 1:1 foam contains mainly closed cell content of 1mm length or less while the 1:2 NIPU sample contains more open cell content of larger 2 mm length cells. Open cell content increases with NIPU 1:2 given the additional amount of low viscosity dimer diamine added in this formulation. More cellular rupture occurs as the lamellar layer is thinner with lower viscosity reaction mixtures.<sup>58</sup> Given that the nonporous NIPU material has a density of

approximately  $1000 \text{ kg/m}^3$  for both NIPU 1:1 and 1:2, the porosity ( $\phi$ ) and volume expansion ( $\Phi$ ) of the foamed materials can be calculated according to equation 4 and 5 respectively:

$$\phi = 1 - (\rho_f / \rho_m) \quad (4)$$

$$\Phi = \rho_m / \rho_f \quad (5)$$

where  $\rho_m$  is the density of the original material and  $\rho_f$  that of the foamed material. Results shown in Table 4 reflect an over 4-fold increase in volume during the foaming reaction corresponding to porosity values of around 0.75. These results correlate well with a foaming study using PMHS on biobased epoxy foams published by our lab.<sup>59</sup>

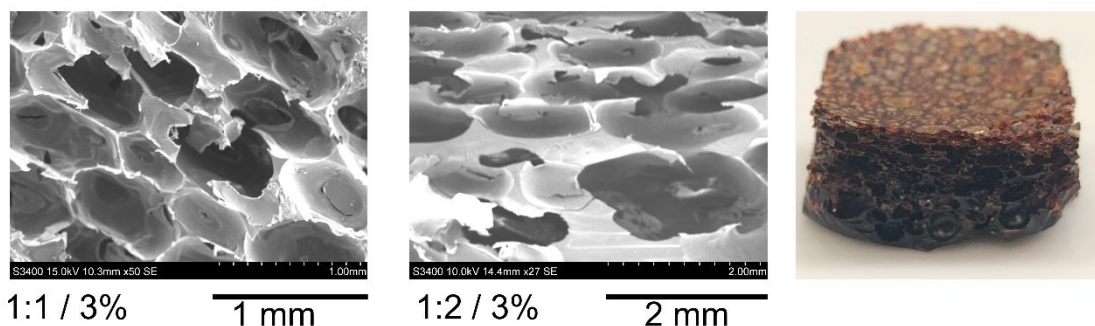


**Figure 9:** SEM images of NIPU foams. A stoichiometric amount of diamine leads to mostly closed cell content in NIPU 1:1(left) whereas excess diamine creates an open cell morphology in NIPU 1:2 (right). Far right, example of a NIPU foam of density  $\sim 300 \text{ kg/m}^3$ .

Finally, the biobased content of the NIPU foam was measured by the services of a proprietary analytical lab following ASTM D6866 for determination of the biobased content of a polymer sample using radiocarbon analysis<sup>60</sup>. The analysis determines the

percent modern carbon (pMC) content by measuring the  $^{14}\text{C} / \text{C}^{12}$  ratio of a sample and comparing to a standard with known bio-content established by the National Institute of Standards and Technology (NIST)<sup>60</sup>. The composition of the NIPU foam contains biobased components from the lignin, curing agent, and potentially the organic carbonate reagents used to oxyalkylate and cyclocarbonate the lignin precursors. The only non-biobased components reside in the use of the catalyst (TBD) and foaming agent (PMHS). The analysis from radiocarbon dating reported a pMC of  $99.82 \% \pm 0.28 \%$  for the NIPU foam that with a correction factor for atmospheric  $^{14}\text{C}$ , and within experimental error, was reported as containing 100% bio-content. This analysis confirms the biobased origin of the precursor materials and reveals the fate of the foaming agent and catalyst used in the reaction mixture. These two constituents must be evaporated from the sample during the curing reaction given the proximity of their boiling points (TBD:  $222^\circ\text{C}$ , PMHS:  $177^\circ\text{C}$ ) to the curing temperature ( $150^\circ\text{C}$ ). The validation of a 100% biobased NIPU with enhanced mechanical properties is an unprecedented achievement based on the current literature.

## Conclusion

The protocol presented here enables an exceptionally sustainable polyurethane from lignin using biomass as feedstock for both the lignin precursors and curing agent resulting in materials 100% biobased carbon content. In addition, a unique non-toxic cyclocarbonation scheme was utilized for the first time on Kraft lignin leading to the creation of NIPUs with comparable properties to diisocyanate-based PUs. The unique

properties of the lignin- derived NIPUs result from the high reactivity observed between the cyclocarbonates and diamines leading to rapid gelation of the reaction mixture. The mechanical and structural analysis coincide to reveal a dual phase polymeric structure with tunable properties based on the addition of the aliphatic curing agent.

However, it must be observed that the common issue of lignin-heterogeneity can be witnessed by the often-large standard deviations associated with the results from tensile and compression testing. In addition, the storage modulus reflected in the DMA analysis shows a large temperature transition region between the glassy and rubbery state possibly indicating many microstates of polymeric material. Given the PDI of the CC lignin precursors of 4.1, it is hypothesized that a range of molecular weights in the cured material is largely responsible for this behavior. Diisocyanate-based PUs employing lignin have shown a range of properties based on the molecular weight of lignin precursors. The use of industrial Kraft lignin in this study sacrifices precision in molecular weight for efficiency and sustainability in processing.

The success of the reaction scheme is supported by the impressive mechanical properties of the NIPU and foamed samples as well as the shape memory characteristics demonstrated in this report. This study is an example that the biorefinery concept of the future can make use of less precise starting material<sup>62</sup> to synthesize unique and high performing materials to replace traditional materials with heavy environmental burdens. The simplicity and non-toxicity of the protocol presented here overcomes some of the main hurdles with regard to lignin chemistry: low reactivity, solubility and compatibility with curing agents, and excessively brittle structures unable to undergo mechanical

characterization. Therefore, starting from this study, it is possible to envision optimization studies targeting more specific physical and mechanical properties using smaller molecular weight ranges through lignin fractionation and depolymerization.

### Acknowledgements

The authors would like to thank Olivia Sequerth of Clemson University for her support in synthesizing lignin precursors and Graham Tindall of Clemson University for performing GPC on lignin precursors. The authors would like to thank Dr. Johannes Leisen of Georgia Tech University for performing CP/MAS SS NMR analysis and Kimberly Ivey of Clemson University for performing FTIR, DMA and TGA analysis. The authors would also like to acknowledge financial support by DOE Award# 0000253812, Robert Patrick Jenkins Professorship, and Dean's Faculty Fellow Professorship. J.S. also wishes to acknowledge the partial financial support provided by the Cooper-Standard Fellowship, Draexlmaier Fellowship and Sonoco Fellowship.

### Conflict of Interest

The authors declare no conflict of interest.

### References

- (1) Ragauskas, A. J.; Beckham, G. T.; Biddy, M. J.; Chandra, R.; Chen, F.; Davis, M. F.; Davison, B. H.; Dixon, R. A.; Gilna, P.; Keller, M.; et al. Lignin Valorization: Improving Lignin Processing in the Biorefinery. *Science*. 2014.
- (2) Upton, B. M.; Kasko, A. M. Strategies for the Conversion of Lignin to High-Value Polymeric Materials: Review and Perspective. *Chem. Rev.* **2016**, *116* (4), 2275–2306.
- (3) Duval, A.; Lawoko, M. A Review on Lignin-Based Polymeric, Micro- and Nano-Structured Materials. *React. Funct. Polym.* **2014**, *85*, 78–96.
- (4) Laurichesse, S.; Avérous, L. Chemical Modification of Lignins: Towards Biobased Polymers. *Prog. Polym. Sci.* **2014**, *39* (7), 1266–1290.
- (5) Gama, N.; Ferreira, A.; Barros-Timmons, A.; Gama, N. V.; Ferreira, A.; Barros-Timmons, A. Polyurethane Foams: Past, Present, and Future. *Materials (Basel)*. **2018**, *11* (10), 1841.
- (6) Lithner, D.; Larsson, Å.; Dave, G. Environmental and Health Hazard Ranking and Assessment of Plastic Polymers Based on Chemical Composition. *Sci. Total Environ.* **2011**, *409* (18), 3309–3324.
- (7) Li, Y.; Ragauskas, A. J. Kraft Lignin-Based Rigid Polyurethane Foam. *J. Wood Chem. Technol.* **2012**, *32* (3), 210–224.
- (8) Mahmood, N.; Yuan, Z.; Schmidt, J.; Xu, C. (Charles). Preparation of Bio-Based

- Rigid Polyurethane Foam Using Hydrolytically Depolymerized Kraft Lignin via Direct Replacement or Oxypropylation. *Eur. Polym. J.* **2015**, *68*, 1–9.
- (9) Cateto, C. A.; Barreiro, M. F.; Rodrigues, A. E.; Belgacem, M. N. Optimization Study of Lignin Oxypropylation in View of the Preparation of Polyurethane Rigid Foams. *Ind. Eng. Chem. Res.* **2009**, *48* (5), 2583–2589.
- (10) Liu, L.-Y.; Cho, M.; Sathitsuksanoh, N.; Chowdhury, S.; Renneckar, S. Uniform Chemical Functionality of Technical Lignin Using Ethylene Carbonate for Hydroxyethylation and Subsequent Greener Esterification. *ACS Sustain. Chem. Eng.* **2018**, *6* (9), 12251–12260.
- (11) Kühnel, I.; Podschun, J.; Saake, B.; Lehnen, R. Synthesis of Lignin Polyols via Oxyalkylation with Propylene Carbonate. *Holzforschung* **2015**, *69* (5), 531–538.
- (12) Kühnel, I.; Saake, B.; Lehnen, R. Oxyalkylation of Lignin with Propylene Carbonate: Influence of Reaction Parameters on the Ensuing Bio-Based Polyols. *Ind. Crops Prod.* **2017**, *101* (101), 75–83.
- (13) Kühnel, I.; Saake, B.; Lehnen, R. Comparison of Different Cyclic Organic Carbonates in the Oxyalkylation of Various Types of Lignin. *React. Funct. Polym.* **2017**, *120*, 83–91.
- (14) Duval, A.; Avérous, L. Cyclic Carbonates as Safe and Versatile Etherifying Reagents for the Functionalization of Lignins and Tannins. *ACS Sustain. Chem. Eng.* **2017**, *5* (8), 7334–7343.
- (15) Over, L. C.; Meier, M. A. R. Sustainable Allylation of Organosolv Lignin with Diallyl Carbonate and Detailed Structural Characterization of Modified Lignin. *Green Chem.* **2016**, *18* (1), 197–207.
- (16) Rokicki, G.; Parzuchowski, P. G.; Mazurek, M. Non-Isocyanate Polyurethanes: Synthesis, Properties, and Applications. *Polym. Adv. Technol.* **2015**, *26* (7), 707–761.
- (17) Kathalewar, M. S.; Joshi, P. B.; Sabnis, A. S.; Malshe, V. C. Non-Isocyanate Polyurethanes: From Chemistry to Applications. *RSC Adv.* **2013**, *3* (13), 4110.
- (18) Błażek, K.; Datta, J. Renewable Natural Resources as Green Alternative Substrates to Obtain Bio-Based Non-Isocyanate Polyurethanes-Review. *Crit. Rev. Environ. Sci. Technol.* **2019**, *49* (3), 173–211.
- (19) Kühnel, I.; Saake, B.; Lehnen, R. A New Environmentally Friendly Approach to Lignin-Based Cyclic Carbonates. *Macromol. Chem. Phys.* **2018**, *219* (7), 1700613.
- (20) Javni, I.; Hong, D. P.; Petrović, Z. S. Soy-Based Polyurethanes by Nonisocyanate Route. *J. Appl. Polym. Sci.* **2008**, *108* (6), 3867–3875.
- (21) Esmaili, N.; Zohuriaan-Mehr, M. J.; Salimi, A.; Vafayan, M.; Meyer, W. Tannic Acid Derived Non-Isocyanate Polyurethane Networks: Synthesis, Curing Kinetics, Antioxidizing Activity and Cell Viability. *Thermochim. Acta* **2018**, *664*, 64–72.
- (22) Maisonneuve, L.; More, A. S.; Foltran, S.; Alfos, C.; Robert, F.; Landais, Y.; Tassaing, T.; Grau, E.; Cramail, H. Novel Green Fatty Acid-Based Bis-Cyclic Carbonates for the Synthesis of Isocyanate-Free Poly(Hydroxyurethane Amide)s. *RSC Adv.* **2014**, *4* (49), 25795–25803.
- (23) Zhang, K.; Nelson, A. M.; Talley, S. J.; Chen, M.; Margareta, E.; Hudson, A. G.; Moore, R. B.; Long, T. E. Non-Isocyanate Poly(Amide-Hydroxyurethane)s from

- Sustainable Resources. *Green Chem.* **2016**, *18* (17), 4667–4681.
- (24) Lee, A.; Deng, Y. Green Polyurethane from Lignin and Soybean Oil through Non-Isocyanate Reactions. *Eur. Polym. J.* **2015**, *63*, 67–73.
- (25) Salanti, A.; Zoia, L.; Orlandi, M. Chemical Modifications of Lignin for the Preparation of Macromers Containing Cyclic Carbonates. *Green Chem.* **2016**, *18* (14), 4063–4072.
- (26) Salanti, A.; Zoia, L.; Mauri, M.; Orlandi, M. Utilization of Cyclocarbonated Lignin as a Bio-Based Cross-Linker for the Preparation of Poly(Hydroxy Urethane)S. *RSC Adv.* **2017**, *7* (40), 25054–25065.
- (27) Mimini, V.; Amer, H.; Hettegger, H.; Bacher, M.; Gebauer, I.; Bischof, R.; Fackler, K.; Potthast, A.; Rosenau, T. Lignosulfonate-Based Polyurethane Materials via Cyclic Carbonates: Preparation and Characterization. *Holzforschung* **2020**, *74* (2), 203–211.
- (28) Grignard, B.; Thomassin, J.-M.; Gennen, S.; Poussard, L.; Bonnaud, L.; Raquez, J.-M.; Dubois, P.; Tran, M.-P.; Park, C. B.; Jerome, C.; et al. CO<sub>2</sub>-Blown Microcellular Non-Isocyanate Polyurethane (NIPU) Foams: From Bio- and CO<sub>2</sub>-Sourced Monomers to Potentially Thermal Insulating Materials. *Green Chem.* **2016**, *18* (7), 2206–2215.
- (29) Xi, X.; Pizzi, A.; Gerardin, C.; Lei, H.; Chen, X.; Amirou, S. Preparation and Evaluation of Glucose Based Non-Isocyanate Polyurethane Self-Blowing Rigid Foams. *Polymers (Basel)*. **2019**, *11* (11), 1802.
- (30) Cornille, A.; Dworakowska, S.; Bogdal, D.; Boutevin, B.; Caillol, S. A New Way of Creating Cellular Polyurethane Materials: NIPU Foams. *Eur. Polym. J.* **2015**, *66*, 129–138.
- (31) Cornille, A.; Guillet, C.; Benyahya, S.; Negrell, C.; Boutevin, B.; Caillol, S. Room Temperature Flexible Isocyanate-Free Polyurethane Foams. *Eur. Polym. J.* **2016**, *84*, 873–888.
- (32) Federation of European Rigid Polyurethane Foam Associations. *Thermal Insulation Materials Made of Rigid Polyurethane Foam (PUR/PIR) Properties-Manufacture*; Brussels, Belgium, 2006.
- (33) Granata, A.; Argyropoulos, D. S. 2-Chloro-4,4,5,5-Tetramethyl-1,3>2-Dioxaphospholane, a Reagent for the Accurate Determination of the Uncondensed and Condensed Phenolic Moieties in Lignins. *J. Agric. Food Chem.* **1995**, *43*, 1538–1544.
- (34) Schutyser, W.; Renders, T.; Van den Bosch, S.; Koelewijn, S.-F.; Beckham, G. T.; Sels, B. F. Chemicals from Lignin: An Interplay of Lignocellulose Fractionation, Depolymerisation, and Upgrading. *Chem. Soc. Rev.* **2018**, *47* (3), 852–908.
- (35) Duval, C.; Kébir, N.; Jauseau, R.; Burel, F. Organocatalytic Synthesis of Novel Renewable Non-Isocyanate Polyhydroxyurethanes. *J. Polym. Sci. Part A Polym. Chem.* **2016**, *54* (6), 758–764.
- (36) Carré, C.; Bonnet, L.; Avérous, L. Original Biobased Nonisocyanate Polyurethanes: Solvent- and Catalyst-Free Synthesis, Thermal Properties and Rheological Behaviour. *RSC Adv.* **2014**, *4* (96), 54018–54025.
- (37) Poussard, L.; Mariage, J.; Grignard, B.; Detrembleur, C.; Jérôme, C.; Calberg, C.;

- Heinrichs, B.; De Winter, J.; Gerbaux, P.; Raquez, J.-M.; et al. Non-Isocyanate Polyurethanes from Carbonated Soybean Oil Using Monomeric or Oligomeric Diamines To Achieve Thermosets or Thermoplastics. *Macromolecules* **2016**, *49* (6), 2162–2171.
- (38) Rix, E.; Grau, E.; Chollet, G.; Cramail, H. Synthesis of Fatty Acid-Based Non-Isocyanate Polyurethanes, NIPUs, in Bulk and Mini-Emulsion. *Eur. Polym. J.* **2016**, *84*, 863–872.
- (39) Martin, A.; Lecamp, L.; Labib, H.; Aloui, F.; Kébir, N.; Burel, F. Synthesis and Properties of Allyl Terminated Renewable Non-Isocyanate Polyurethanes (NIPUs) and Polyureas (NIPUreas) and Study of Their Photo-Crosslinking. *Eur. Polym. J.* **2016**, *84*, 828–836.
- (40) Hatakeyama, H.; Hatakeyama, T. Environmentally Compatible Hybrid-Type Polyurethane Foams Containing Saccharide and Lignin Components. *Macromol. Symp.* **2005**, *224* (1), 219–226.
- (41) Avelino, F.; Almeida, S. L.; Duarte, E. B.; Sousa, J. R.; Mazzetto, S. E.; de Souza Filho, M. de S. M. Thermal and Mechanical Properties of Coconut Shell Lignin-Based Polyurethanes Synthesized by Solvent-Free Polymerization. *J. Mater. Sci.* **2018**, *53* (2), 1470–1486.
- (42) Matsushita, Y.; Inomata, T.; Takagi, Y.; Hasegawa, T.; Fukushima, K. Conversion of Sulfuric Acid Lignin Generated during Bioethanol Production from Lignocellulosic Materials into Polyesters with  $\epsilon$ -Caprolactone. *J. Wood Sci.* **2011**, *57* (3), 214–218.
- (43) Sun, Y.; Yang, L.; Lu, X.; He, C. Biodegradable and Renewable Poly(Lactide)–Lignin Composites: Synthesis, Interface and Toughening Mechanism. *J. Mater. Chem. A* **2015**, *3* (7), 3699–3709.
- (44) Datta, J.; Włoch, M. Progress in Non-Isocyanate Polyurethanes Synthesized from Cyclic Carbonate Intermediates and Di- or Polyamines in the Context of Structure–Properties Relationship and from an Environmental Point of View. *Polym. Bull.* **2016**, *73* (5), 1459–1496.
- (45) Nohra, B.; Candy, L.; Blanco, J.-F.; Guerin, C.; Raoul, Y.; Mouloungui, Z. From Petrochemical Polyurethanes to Biobased Polyhydroxyurethanes. *Macromolecules* **2013**, *46* (10), 3771–3792.
- (46) Lu, Y.; Lu, Y.-C.; Hu, H.-Q.; Xie, F.-J.; Wei, X.-Y.; Fan, X. Structural Characterization of Lignin and Its Degradation Products with Spectroscopic Methods. **2017**.
- (47) Bähr, M.; Bitto, A.; Mülhaupt, R. Cyclic Limonene Dicarboxylate as a New Monomer for Non-Isocyanate Oligo- and Polyurethanes (NIPU) Based upon Terpenes. *Green Chem.* **2012**, *14* (5), 1447.
- (48) Pu, Y.; Hallac, B.; Ragauskas, A. J. *Plant Biomass Characterization: Application of Solution- and Solid-State NMR Spectroscopy*.
- (49) Laurichesse, S.; Huillet, C.; Avérous, L. Original Polyols Based on Organosolv Lignin and Fatty Acids: New Bio-Based Building Blocks for Segmented Polyurethane Synthesis. *Green Chem.* **2014**, *16* (8), 3958–3970.
- (50) Tavares, L.; Schleder, G. R. Bio-Based Polyurethane Prepared from Kraft Lignin



and Modified Castor Oil.

- (51) Hatakeyama, T.; Izuta, Y.; Hirose, S.; Hatakeyama, H. Phase Transitions of Lignin-Based Polycaprolactones and Their Polyurethane Derivatives. *Polymer (Guildf)*. **2002**, *43* (4), 1177–1182.
- (52) Liu, C.; Qin, H.; Mather, P. T. Review of Progress in Shape-Memory Polymers. *J. Mater. Chem.* **2007**, *17* (16), 1543–1558.
- (53) Nissenbaum, A.; Greenfeld, I.; Wagner, H. D. Shape Memory Polyurethane - Amorphous Molecular Mechanism during Fixation and Recovery. *Polymer (Guildf)*. **2020**, *190*, 122226.
- (54) Li, Y.; Ragauskas, A. J. Kraft Lignin-Based Rigid Polyurethane Foam. *J. Wood Chem. Technol.* **2012**, *32* (3), 210–224.
- (55) Blattmann, H.; Lauth, M.; Mülhaupt, R.; Blattmann, H.; Mülhaupt, R.; Lauth, M. Flexible and Bio-Based Nonisocyanate Polyurethane (NIPU) Foams. **2016**.
- (56) Thirumal, M.; Khastgir, D.; Singha, N. K.; Manjunath, B. S.; Naik, Y. P. Effect of Foam Density on the Properties of Water Blown Rigid Polyurethane Foam. *J. Appl. Polym. Sci.* **2008**, *108* (3), 1810–1817.
- (57) Huo, S.-P.; Nie, M.-C.; Kong, Z.-W.; Wu, G.-M.; Chen, J. Crosslinking Kinetics of the Formation of Lignin-Aminated Polyol-Based Polyurethane Foam. *J. Appl. Polym. Sci.* **2012**, *125* (1), 152–157.
- (58) Lau, T. H. M.; Wong, L. L. C.; Lee, K.-Y.; Bismarck, A. Tailored for Simplicity: Creating High Porosity, High Performance Bio-Based Macroporous Polymers from Foam Templates. *Green Chem.* **2014**, *16* (4), 1931–1940.
- (59) Brown, N. F.; Pradeep, S. A.; Agnihotri, S.; Pilla, S. The Power of Processing: Creating High Strength Foams from Epoxidized Pine Oil. *ACS Sustain. Chem. Eng.* **2017**, *5* (10), 8641–8647.
- (60) *ASTM6866: Standard Test Methods for Determining the Biobased Content of Solid, Liquid, and Gaseous Samples Using Radiocarbon Analysis.*
- (61) Pan, X.; Sengupta, P.; Webster, D. C. High Biobased Content Epoxy–Anhydride Thermosets from Epoxidized Sucrose Esters of Fatty Acids. *Biomacromolecules* **2011**, *12* (6), 2416–2428.
- (62) Llevot, A.; Dannecker, P.-K.; von Czapiewski, M.; Over, L. C.; Söyler, Z.; Meier, M. A. R. Renewability Is Not Enough: Recent Advances in the Sustainable Synthesis of Biomass-Derived Monomers and Polymers. *Chem. - A Eur. J.* **2016**, *22* (33), 11510–11521.

